

# Enhancement of nucleate boiling heat transfer by micro-structured chromium nitride surfaces

S. Fischer<sup>1,4</sup>, E. M. Slomski<sup>2</sup>, P. Stephan<sup>1,3</sup> and M. Oechsner<sup>2</sup>

<sup>1</sup> Institute for Technical Thermodynamics, Technische Universität Darmstadt, Petersenstr. 32, D-64287 Darmstadt, Germany, phone: +49 6151/16-4464, fax: +49 6151/16-6561

<sup>2</sup> State Material Testing Institute Darmstadt, Institute for Material Technology, Surface Technology and Corrosion, Technische Universität Darmstadt, Grafenstr. 2, D-64283 Darmstadt, Germany, phone: +49 6151/16-4441, fax: +49 6151/16-4170

<sup>3</sup>Center of Smart Interfaces, Technische Universität Darmstadt, Petersenstr. 32, D-64287 Darmstadt, Germany

E-mail: [fischer@ttd.tu-darmstadt.de](mailto:fischer@ttd.tu-darmstadt.de)

**Abstract.** In the present work, the influence of micro-structured chromium nitride (CrN) surfaces on boiling heat transfer during nucleate boiling of FC-72 at saturation temperature was investigated. The CrN thin coatings of 4.5  $\mu\text{m}$  thickness in average were deposited by Physical Vapor Deposition (PVD) as a combination of High Power Impulse Magnetron Sputtering (HiPIMS) and Direct Current Magnetron Sputtering (DCMS) on polished copper surfaces. Due to variation of the applied bias voltage to the substrates different sizes and orientations of the CrN crystals were realized. The typical dimensions of the hereby generated surface structures are in the order of a few hundred nm to a few  $\mu\text{m}$ . It was found that all employed micro-structured CrN surfaces yield an increase of the critical heat flux (CHF) compared to an uncoated reference surface. The maximum ratio of the CHF of a CrN structured surface to the CHF of the uncoated copper surface reached within this study was  $\text{CHF}_{\text{max}}/\text{CHF}_{\text{ref}} = 2.5$ .

## List of Symbols

$A$	area	$[\text{m}^2]$
$h$	heat transfer coefficient	$[\text{W}/\text{m}^2\text{K}]$
$p$	pressure	$[\text{mbar}]$
$Q$	heat flow	$[\text{W}]$
$q$	heat flux	$[\text{W}/\text{m}^2]$
$s$	distance from the heater surface	$[\text{m}]$
$t$	temperature	$[\text{°C}]$
$t_{\text{sat}}$	saturation temperature	$[\text{°C}]$
$t_{\text{fluid}}$	fluid temperature	$[\text{°C}]$
$t_{\text{wall}}$	heater surface temperature	$[\text{°C}]$
$U_{\text{bias}}$	coating process bias voltage	$[\text{V}]$
$U_{\text{booster}}$	coating process booster voltage	$[\text{V}]$
$\Delta T_{\text{W}}$	wall superheat	$[\text{K}]$

<sup>4</sup> to whom any correspondence should be adressed

## 1. Introduction

Boiling is a highly efficient heat transfer mechanism and plays an important role in many technical applications due to its high realizable heat transfer coefficients. The generation of vapor bubbles on heated surfaces primarily takes place at microscopic imperfections of the surface referred to as nucleation sites. One possibility to increase the overall heat transfer in nucleate boiling is to increase the number of active nucleation sites at the heater surface. Numerous studies show an enhancement of the critical heat flux (CHF) and the heat transfer coefficient (HTC) of micro- and nano-structured surfaces in comparison to a smooth reference surface. A review of experimental work on boiling on structured surfaces is given by Honda and Wei [1]. Micro-structured surfaces can be generated for example by application of particles onto the heater surface [2, 3] or by microelectronic fabrication techniques such as dry etching [4] or micro-electro mechanical systems (MEMS) [5]. Hendricks et al. [6] used a Microreactor-assisted nanomaterial deposition technique to create both hydrophilic and superhydrophilic nano-structured ZnO surfaces. Surface modifications in the same order of magnitude have been achieved by El-Genk and Ali [7] through an electro-chemical deposition technique.

Such micro- and nano-structured surfaces can be subjected to large local pressure gradients induced by the moving phase-boundaries that can result in degradation of the surface structure if exposed to long term boiling conditions [8]. An approach to mitigate this circumstance for industrial applications is the deposition of highly durable microstructures by Physical Vapor Deposition (PVD). Chromium nitride PVD thin coatings are typically used as wear protection coatings for cutting tools and exhibit high mechanical resistance and good adhesion properties. The crystal structure, morphology and topography of magnetron sputtered thin coatings can be influenced by the process parameters during deposition [9]. A hybrid process consisting of High Power Impulse Magnetron Sputtering (HiPIMS) and Direct Current Magnetron Sputtering (DCMS) ensures high control of the crystal growth and at the same time a sufficient deposition rate [10, 11].

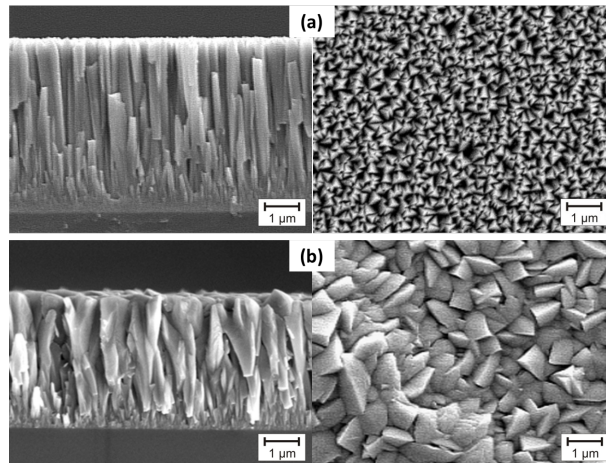


**Figure 1.** SEM cross-view picture of notched specimen (left) and SEM top view picture of the surface structure (right)

In figure 1 two differently microstructured CrN coatings are shown ((a) bias voltage  $U_{\text{bias}} = 0$  V, (b) bias voltage  $U_{\text{bias}} = -100$  V). This example shows that especially the bias voltage applied to the substrates during the deposition process can be used to change surface morphology of the CrN coating. A closer description of the coating process and the coating parameters covered in this study is given in section 3. The boiling process on the differently coated

surfaces was investigated using a boiling test cell as described in section 2. From the measured temperature data heater surface temperatures, heat fluxes, and heat transfer coefficients have been calculated for four CrN coated copper samples deposited at different bias voltages and one polished copper reference surface according to the methods described in section 4. The results of these measurements are discussed in section 5. Finally in section 6 a summary and conclusion is given.

## 2. Experiment setup

A schematic of the experiment setup is displayed in figure 2. The experiments were conducted using the electronic cooling fluid FC-72, which was properly degassed in-situ before each experiment run. All experiment runs were conducted at a pressure of  $p = 1013$  mbar, which was established over an elastic membrane. The liquid was kept at saturation temperature  $t_{\text{sat}} = 56.6$  °C with a thermostat, that flowed through the test cell walls. The liquid temperature  $t_{\text{fluid}}$  was measured at 3 different heights within the test cell and showed throughout all experiment runs little deviation from the saturation temperature ( $\pm 0.1$  °C). From below the coated copper samples were inserted into the test cell (more information on the coating process and the coating parameters is given in section 3).

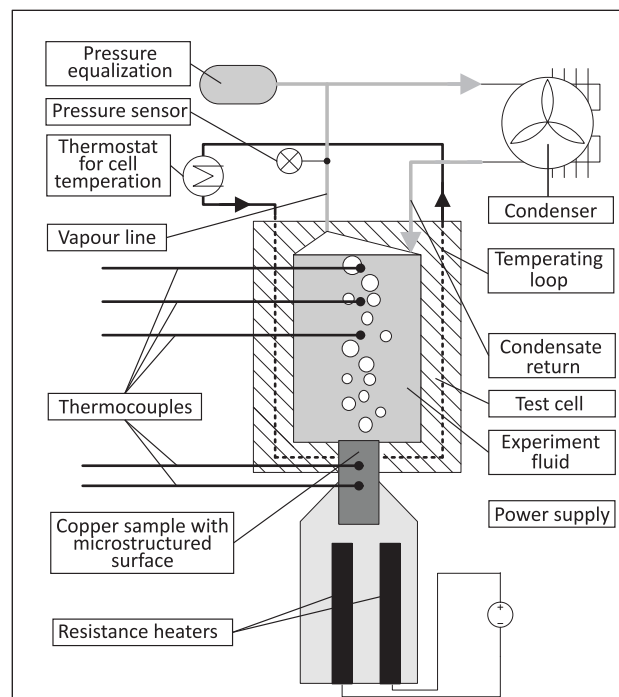


**Figure 2.** Schematic experimental setup

The copper samples were connected to the test cell using a polycarbonate frame which the sample was glued into to avoid heat conduction between copper sample and test cell wall. The samples were heated from below through a screwed-on copper heating element equipped with 4 heater cartridges with a maximum power of 100 W each. Voltage and current supplied to the heater cartridges was permanently logged by the measurement system to determine the input power. However, to eliminate heat losses from the measured values, the heat flux supplied to the coated sample surface was determined differently, as closer described in section 4. Copper

sample and heater element were thermally insulated by a surrounding Teflon block to minimize radial thermal losses. Liquid evaporated through nucleate boiling at the coated copper was fed to a condenser which was cooled passively through a heat pipe cooler. Recondensed liquid was fed from the condenser back into the test cell.

### 3. Coating procedure and parameters

The CrN thin coatings were sputtered onto pure copper substrates by a combined DCMS and HiPIMS process. Prior to the deposition, the substrates were cleaned in a multi-stage ultrasonic bath using ethanol, isopropanol and n-heptane as cleaning fluids without intermediate drying. Additionally, all specimens were heated up and cleaned by mf-sputter etching prior to the deposition process. Finally the coating took place by reactive magnetron sputtering in a nitrogen/argon gas ratio of 60% and a total chamber pressure of 450 mPa. The sputtering targets were formed of pure chromium (99.8%) and the target to sample distance was about 120 mm. To enhance adhesion of the CrN top layer, a pure Chromium interlayer was deposited previously with a coating duration of 180 s. Total target power of the unpulsed DCMS and pulsed HiPIMS-cathode were set at a maximum of 2500 W. According to the applied target power the pulse frequency and pulse length of the HiPIMS-cathode was fixed to 200  $\mu$ s and 100 Hz, respectively.

**Table 1.** Varied coating parameters (parameter ranges refer to a ramp function)

Heater sample No.	Bias Voltage $-U_{\text{bias}}$ [V]
1	50-100
2	50
3	100
4	0

Based on earlier research results, bias voltage was varied to deposit coatings with different crystal structures [9, 12] as given in table 1. The applied bias voltage, either as a ramp function or at constant values (see table 1), lead to differently structured CrN coatings morphology as depicted in figure 3. While a constant low or zero bias voltage, as well as a slowly increasing bias voltage leads to a fine and strictly columnar grain growth perpendicular to the copper sample surfaces (Heater sample No. 1, 2 and 4 in figure 3), an applied constant bias voltage of - 100 V lead to a rather V-shaped grain growth resulting in larger triangular grain tips (Heater sample No. 3 in figure 3).

### 4. Measurement procedure and data reduction

The liquid temperature  $t_{\text{fluid}}$  was measured at three different heights within the test cell using three type K thermocouples. The temperature within the rotationally symmetric coated copper samples was measured at five locations as given in table 2. All thermocouples have been calibrated to provide a relative measurement accuracy of  $\pm 0.15$   $^{\circ}$ C prior to the experiments. Thermocouples 2 and 3 were used to calculate heat flux, heater surface temperature and heat transfer coefficient. Thermocouple 1 was installed to monitor the surface temperature for safety reasons, but since its position is not accurately known, it is not used for any calculations. Thermocouples 4 and 5 were installed in at a radial distance of 5 mm to the central axis of the sample (half its radius) in the same measurement plane as thermocouples 2 and 3, in an attempt to

Heater sample No. 1    Heater sample No. 2    Heater sample No. 3    Heater sample No. 4

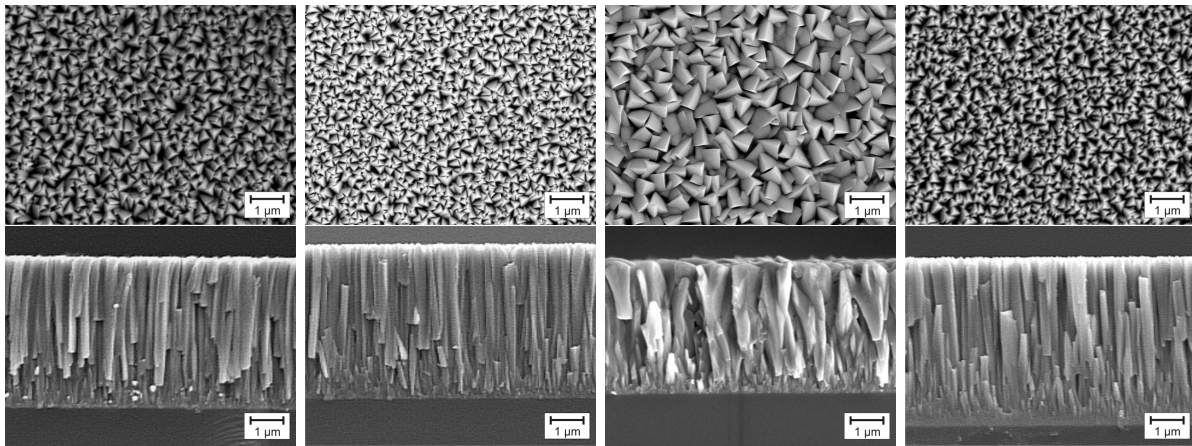


**Figure 3.** SEM images of CrN coatings in top view (upper row) and cross view (lower row) for coating parameter set 1 to 4 as defined in table 1

measure radial heat losses despite the insulation by the teflon block. However, it was found that in all configurations in both measurement planes the temperature homogeneity is far better than measurement uncertainty. Therefore radial heat losses at the heater sample can be neglected and heat conduction within the sample can be assumed to be one-dimensional.

**Table 2.** Position of thermocouples within the heater samples

Thermocouple No.	distance from heater surface $s$ [mm]	distance from central axis [mm]
1	ca. 0.5	0
2	15.5	0
3	30.5	0
4	15.5	5
5	30.5	5

During the experiments the heating power was gradually increased and measurements were taken when steady state was achieved. The temperatures in steady state were recorded by the measurement software (National Instruments LabVIEW) with a measurement frequency of 2000 Hz over a measurement interval of 10 seconds at each measurement point. To reduce measurement noise, the temperatures were averaged over the measurement interval for evaluation. Heating power provided through the heating element was gradually increased until critical heat flux was reached, which was characterized by a strong increase of the heater temperatures.

From thermocouple temperatures 2 and 3 the heat flux is calculated using the following equation:

$$q = \frac{Q}{A} = \frac{\lambda}{(s_3 - s_2)}(t_3 - t_2) \quad (1)$$

Errors of the heat flux calculation have been evaluated to be below  $\pm 7.83 \text{ kW/m}^2$  for all

measured data (linear error propagation). As it heat conduction has been proven to be one-dimensional in the stationary case, the surface temperature  $t_{\text{wall}}$  can be linearly extrapolated from thermocouple temperatures 2 and 3:

$$t_{\text{wall}} = t_2 - \frac{s_2}{(s_3 - s_2)}(t_3 - t_2) \quad (2)$$

Errors of the surface temperature calculation have been evaluated to be below  $\pm 0.46$  °C for all measured data (linear error propagation). From heater wall temperature  $t_{\text{wall}}$  (eq. 2) and heat flux (eq. 1) the heat transfer coefficient is calculated:

$$h = \frac{q}{t_{\text{wall}} - t_{\text{sat}}} \quad (3)$$

Errors of the heat transfer coefficient calculation have been evaluated to be below  $\pm 492.2$  W/m<sup>2</sup>K for all measured data (linear error propagation).

## 5. Results

In figure 4 the boiling curves for the five heater samples are shown along with an uncoated, polished reference copper surface. Arrows indicate CHF. After reaching CHF, power was stepwise reduced again. Measurements taken at stationary steps during power reduction showed excellent reproducibility of the lower part of the boiling curves, while there was a slight hysteresis at high heat fluxes. It is assumed, that this is caused by an unstable vapor film with partial rewetting of the surface, which vanishes below a certain heat flux limit, but this could not be confirmed by optical observation. For better readability and comparability only the ascending parts of the data are displayed in figure 4 without error bars.

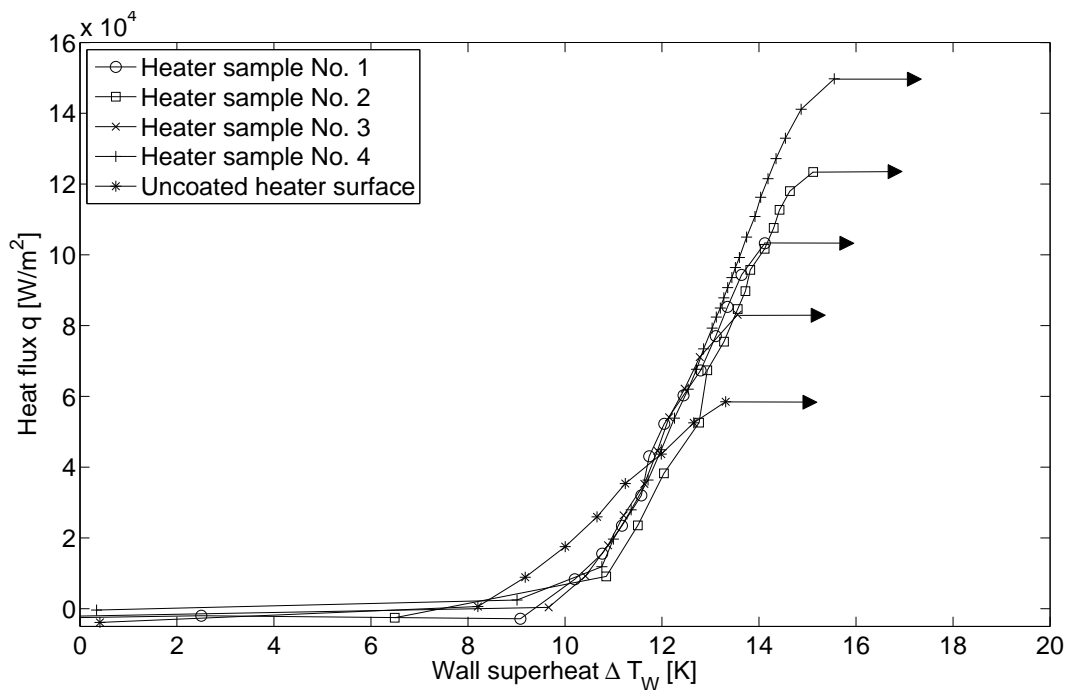


**Figure 4.** boiling curves for the heater samples No. 1 to No. 4 and an uncoated reference heater sample

Measurement errors applicable to figure 4 have been given in section 4. While boiling on the uncoated reference surface starts already at lower wall superheats, the boiling curves of the coated heater samples are much steeper. This indicates a far smaller range of initial phase boundary radii for the coated samples. Some nucleation sites on the uncoated reference surface can be activated easier at lower wall superheats, but an increase of the heater surface temperature increases the number of active nucleation sites only slightly, as the bandwidth of initial phase boundary radii is rather large compared to the coated surfaces. This indicates, that the initial phase boundaries that serve as nucleation sites are rather randomly for the reference surface, while on the coated surface they are determined by the crystalline microstructure. All tested coating parameter variations showed an increase of CHF in comparison to the uncoated surface, up to the factor 2.56 for heater sample no. 4. As general trend it was found that the finer the surface microstructure, the higher the CHF. This becomes clear if one compares the CHF values displayed in figure 4 with the SEM images of the surface microstructure given in figure 3.

In figure 5 the heat transfer coefficients of the coated heater samples and the uncoated reference surface versus the heat flux are displayed. Breakdown of the HTC is indicated by arrows. It can be seen that the coating parameters have little to no influence on the relation of HTC and heat flux. It has however tremendous influence on the point of breakdown of the HTC due to departure from nucleate boiling.

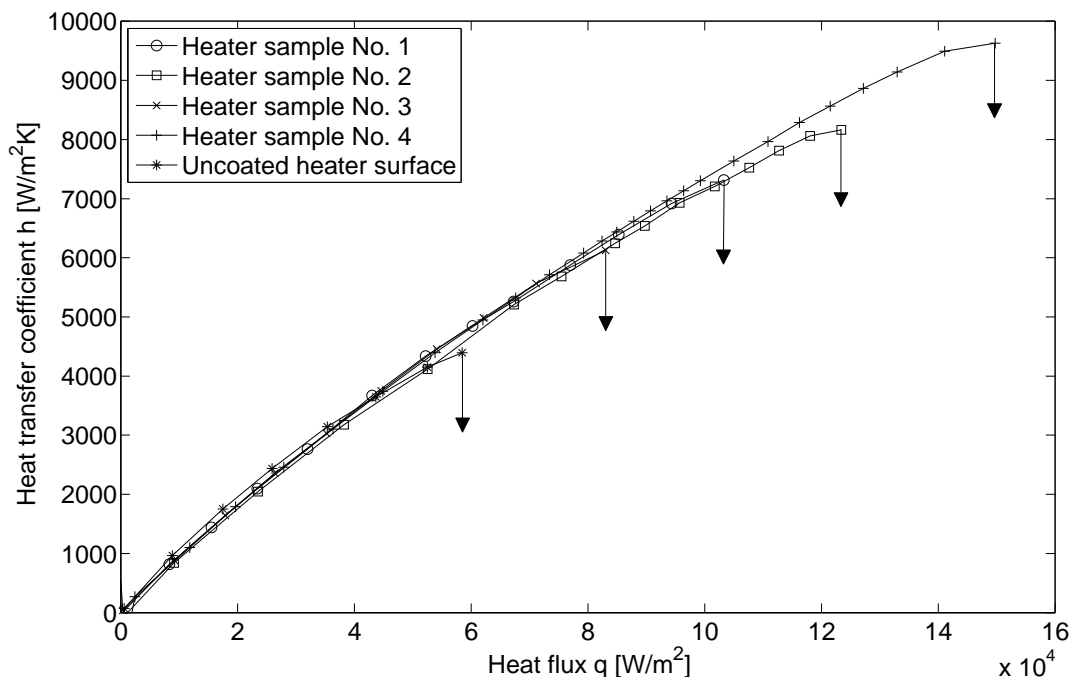


**Figure 5.** Heat transfer coefficients in dependence on the heat flux for the heater samples No. 1 to No. 4 and an uncoated reference heater sample

## 6. Summary and Conclusion

Experiments were performed to investigate heat transfer enhancement during nucleate boiling through application of microstructured chromium nitride thin films onto heater surfaces. Copper

surfaces have been coated by a combination of High Power Impulse Magnetron Sputtering (HiPIMS) and Direct Current Magnetron Sputtering (DCMS) with different coating parameters as given in table 1. The performance of the coated surfaces and an uncoated reference surface were investigated during saturated nucleate boiling of FC-72. While the influence of the surface microstructures onto the relation of HTC and heat flux is negligibly small, each surface increased the maximum HTC and CHF. A summary of the reached values is given in table 3. The increase of CHF and maximum HTC increases with decreasing typical dimensions of the CrN crystal structure. As material wettability is constant for all coatings, it is assumed that the increase in CHF is caused by rewetting of the surface through capillary flow within the surface microstructures.

**Table 3.** Maximum HTC and CHF of the coated heater samples and the uncoated reference sample

Heater sample	CHF [ $\frac{W}{cm^2}$ ]	HTC <sub>max</sub> [ $\frac{W}{m^2K}$ ]
uncoated	5.85	4375.6
No. 1	10.33	7 314.8
No. 2	12.34	8 163.1
No. 3	8.31	6 128.6
No. 4	14.98	9 629.1

Even though the absolute value of CHF reached is far below values measured by Honda et al. [4], the factor between smooth reference surface and maximum reached CHF by the surface modification is equivalent in the present work. The difference in absolute values can be attributed to either different substrates and heating mechanisms (copper in this case heated from below and silicon chips heated by direct joule heating used by Honda et al.) or unknown heat losses, which have not been determined by Honda et al.. The data by Anderson et al. [13], showed extremely high CHF's and are not comparable with the presented data, as all test surfaces in that work were positioned vertically.

It has been shown that microstructured magnetron sputtered CrN thin coatings with high mechanical resistance can be used to increase CHF during nucleate boiling. This method could be suitable for electronic cooling applications where huge fluctuations of heat flux can appear and the surface temperature needs to be kept rather constant (e.g. heater sample no. 4 showed only an increase of the surface temperature of less than 5 K, while the input heat flux was changed from 1 to 14 W/cm<sup>2</sup>).

## References

- [1] Honda H and Wei J 2004 *Exp. Therm. Fluid Sci.* **28** 159 – 169
- [2] Chang J Y and You S M 1997 *Int. J. Heat Mass Transfer* **40** 4437 – 4447
- [3] Hashimoto M, Kasai H, Usami K, Ryoson H, Yazawa K, Weibel J A and Garimella S V 2010 *Proc.14th Int. Heat Transfer Conf.* (Washington D.C.)
- [4] Honda H, Takamastu H and Wei J 2002 *J. Heat Transfer* **124** 383 – 390
- [5] Koizumi Y, Ohtake H and Sato T 2010 *Proc.14th Int. Heat Transfer Conf.* (Washington D.C.)
- [6] Hendricks T, Krishnan S, Choi C, Chang C and Paul B 2010 *Int. J. Heat Mass Transfer* **53** 3357 – 3365
- [7] El-Genk M S and Ali A 2010 *Proc.14th Int. Heat Transfer Conf.* (Washington D.C.)
- [8] Lee C, Bhuiya M and Kim K 2010 *Int. J. Heat Mass Transfer* **53** 4274 – 4279
- [9] Slomski E M, Scheerer H, Trossmann T and Berger C 2010 *Mater. Sci. Technol.* **41** 161 – 165
- [10] Lin J, Wu Z, Zhang X, Mishra B, Moore J and Sproul W 2009 *Thin Solid Films* **517** 18871894
- [11] Lin J, Moore J J, William D Sproul and B M, Wu Z and Wang J 2010 *Surf. Coat. Technol.* **204** 22302239
- [12] Slomski E M, Scheerer H, Tromann T and Berger C 2010 *Surf. Coat. Technol.* **205** 47–50
- [13] Anderson T M and Mudawar I 1989 *J. Heat Transfer* **111** 752 – 759